

# Neutron star structure and collective excitations of finite nuclei

---

Paar, Nils; Moustakidis, Ch. C.; Marketin, Tomislav; Vretenar, Dario; Lalazissis, G. A.

Source / Izvornik: **Physical Review C - Nuclear Physics, 2014, 90**

Journal article, Published version

Rad u časopisu, Objavljena verzija rada (izdavačev PDF)

<https://doi.org/10.1103/PhysRevC.90.011304>

Permanent link / Trajna poveznica: <https://urn.nsk.hr/urn:nbn:hr:217:986039>

Rights / Prava: [In copyright](#)

Download date / Datum preuzimanja: **2022-01-29**



Repository / Repozitorij:

[Repository of Faculty of Science - University of Zagreb](#)



## Neutron star structure and collective excitations of finite nuclei

N. Paar,<sup>1,\*</sup> Ch. C. Moustakidis,<sup>2</sup> T. Marketin,<sup>1</sup> D. Vretenar,<sup>1</sup> and G. A. Lalazissis<sup>2</sup>

<sup>1</sup>*Department of Physics, Faculty of Science, University of Zagreb, Croatia*

<sup>2</sup>*Department of Theoretical Physics, Aristotle University of Thessaloniki, GR-54124 Thessaloniki, Greece*

(Received 28 March 2014; published 24 July 2014)

A method is introduced that establishes relations between properties of collective excitations in finite nuclei and the phase transition density  $n_t$  and pressure  $P_t$  at the inner edge separating the liquid core and the solid crust of a neutron star. A theoretical framework that includes the thermodynamic method, relativistic nuclear energy density functionals, and the quasiparticle random-phase approximation is employed in a self-consistent calculation of  $(n_t, P_t)$  and collective excitations in nuclei. Covariance analysis shows that properties of charge-exchange dipole transitions, isovector giant dipole and quadrupole resonances, and pygmy dipole transitions are correlated with the core-crust transition density and pressure. A set of relativistic nuclear energy density functionals, characterized by systematic variation of the density dependence of the symmetry energy of nuclear matter, is used to constrain possible values for  $(n_t, P_t)$ . By comparing the calculated excitation energies of giant resonances, energy-weighted pygmy dipole strength, and dipole polarizability with available data, we obtain the weighted average values:  $n_t = 0.0955 \pm 0.0007 \text{ fm}^{-3}$  and  $P_t = 0.59 \pm 0.05 \text{ MeV fm}^{-3}$ . This approach crucially depends on experimental results for collective excitations in nuclei and, therefore, accurate measurements are necessary to further constrain the structure of the crust of neutron stars.

DOI: [10.1103/PhysRevC.90.011304](https://doi.org/10.1103/PhysRevC.90.011304)

PACS number(s): 21.60.Jz, 21.65.Ef, 24.30.Cz, 26.60.-c

Probing the structure of the crust of a neutron star presents an important open problem in astrophysics. A solid crust of  $\approx 1$  km thickness, composed of nonuniform neutron-rich matter, is located above a liquid core [1]. The crust presents an interface between observable surface phenomena and the invisible core of the star, and its structure can be related to interesting effects, such as glitches in the rotational period of pulsars, thermal relaxation after matter accretion, quasiperiodic oscillations, and anisotropic surface cooling [2]. The inner crust comprises the region from the density at which neutrons drip out from nuclei, to the inner edge separating the solid crust from the homogeneous liquid core. While the density at which neutrons drip out from nuclei is rather well determined, the transition density at the inner edge is much less certain because of insufficient knowledge of the equation of state of neutron-rich nuclear matter.

The phase transition density  $n_t$  and pressure  $P_t$  at the inner edge separating the liquid core and the solid crust determine some of the key properties of neutron stars. More precisely, the crustal fraction of the moment of inertia of a neutron star depends strongly on the value of  $P_t$ , and less pronounced on  $n_t$ . This fraction is particularly interesting because it can be inferred from observations of pulsar glitches. Additionally, radiation of gravitational waves by a neutron star exhibits a strong dependence on the size of the crust, as well as on the location of the interface between the crust and the core. The structure of the pasta phase of the inner crust, which plays an important role in various static and dynamic properties of a neutron star, also depends on  $n_t$  and consequently on the corresponding equation of state.

A number of theoretical studies have shown that the core-crust transition density and pressure are highly sensitive

to the poorly constrained density dependence of the nuclear matter symmetry energy [3–6]. The symmetry energy that governs the composition of the neutron star crust also determines the thickness of the neutron skin  $r_{np} = r_n - r_p$  in nuclei. In Ref. [3] an inverse correlation was found between the liquid-to-solid phase transition density for neutron-rich matter and the neutron-skin thickness of  $^{208}\text{Pb}$ . Additional correlations between  $r_{np}$  and neutron star properties have also been investigated [7], including the neutron star radii [8], the threshold density at the onset of the direct Urca process [9], and the crustal moment of inertia [7,10]. Correlations between  $r_{np}$  and a variety of neutron star properties have recently been studied using covariance analysis based on energy density functionals [11]. As pointed out by Horowitz and Piekarewicz [3], an accurate measurement of the neutron radius of  $^{208}\text{Pb}$  by means of parity-violating electron scattering may have important implications for the structure of the crust of neutron stars. Recently the parity radius experiment (PREX) provided a model-independent evidence for the neutron skin in  $^{208}\text{Pb}$  [12]. However, since the experimental uncertainty of the PREX neutron-skin thickness is very large ( $r_{np} = 0.33_{-0.18}^{+0.16}$  fm), it will be useful to explore additional experimental constraints for neutron star properties.

The purpose of this Rapid Communication is to establish an alternative method to determine neutron star properties by using collective excitations in finite nuclei that correlate with  $r_{np}$  and provide constraints on the symmetry energy. Of particular importance are the liquid-to-solid transition density and pressure, that is, quantities that determine the inner region of the crust. Recent experimental studies of giant resonances, pygmy dipole resonances, and other modes of excitation in nuclei, yielded a wealth of data that constrain the nuclear symmetry energy and neutron-skin thickness [13]. Since there is a direct relation between the liquid-to-solid transition density and the neutron radius of  $^{208}\text{Pb}$  [3], one expects that an analysis

\*npar@phy.hr

of the collective response of finite nuclei could also provide useful information about the crust of neutron stars. This assumption will be put to the test in a framework that includes the thermodynamic method, relativistic nuclear energy density functionals, and covariance analysis.

To determine the liquid-to-solid transition density for neutron-rich matter, the usual approach is to find the density at which the uniform liquid becomes unstable against small-amplitude density fluctuations, indicating the formation of nuclear clusters. In this way a lower bound to the true transition density  $n_t$  is obtained [14]. The procedures used to determine  $n_t$  include the dynamic method [5,14,15], the thermodynamic method [4,16–18], and the random-phase approximation (RPA) [3]. For the purpose of the present study the thermodynamic method will be employed. The constraint that determines the transition density is given by the inequality [4,16]

$$C(n) = n^2 \frac{d^2 V}{dn^2} + 2n \frac{dV}{dn} + (1 - 2x)^2 \left[ n^2 \frac{d^2 E_{\text{sym}}}{dn^2} + 2n \frac{dE_{\text{sym}}}{dn} - 2 \frac{1}{E_{\text{sym}}} \left( n \frac{dE_{\text{sym}}}{dn} \right)^2 \right] > 0, \quad (1)$$

where  $n$ ,  $V$ ,  $x$  and  $E_{\text{sym}}$ , denote the baryon density, the energy per particle of symmetric nuclear matter, the proton fraction, and the symmetry energy, respectively. The transition density  $n_t$  is determined by solving the equation  $C(n_t) = 0$ , and the corresponding transition pressure reads  $P_t(n_t, x_t) = P_b(n_t, x_t) + P_e(n_t, x_t)$ , where  $P_b$ ,  $P_e$  are the baryon and electron contributions, respectively.  $x_t$  denotes the proton fraction that corresponds to  $n_t$ , and is computed using the condition of  $\beta$  equilibrium [4]. For the analysis of correlations between the transition density and pressure ( $n_t, P_t$ ) and observables that characterize collective excitations in finite nuclei, we consistently employ a relativistic nuclear energy density functional (RNEDF) to compute the energy per particle of symmetric nuclear matter and the symmetry energy, and in the RPA calculation of strength functions in finite nuclei. In this work the universal RNEDF with density-dependent meson-nucleon couplings [19] is used, and excitations in spherical nuclei are analyzed in the relativistic quasiparticle random-phase approximation (RQRPA) [20]. The density dependence of the symmetry energy can be expressed in terms of coefficients of a Taylor expansion around nuclear matter saturation density  $n_0$ :

$$E_{\text{sym}}(n) = E_{\text{sym}}(n_0) + L \left( \frac{n - n_0}{3n_0} \right) + \dots, \quad (2)$$

where  $E_{\text{sym}}(n_0) \equiv J$  is the symmetry energy at saturation, and  $L$  denotes the slope parameter. It has been shown that the parameters  $J, L$  correlate not only with the neutron-skin thickness of nuclei [21,22], but also with neutron star properties [11,23].

To assess the information content on the neutron star liquid-to-solid transition density and pressure of observables that characterize collective excitations in nuclei, the thermodynamic method, the RNEDF, and covariance analysis [24] are used to calculate correlations between quantities of interest. Covariance analysis is the least biased and most complete

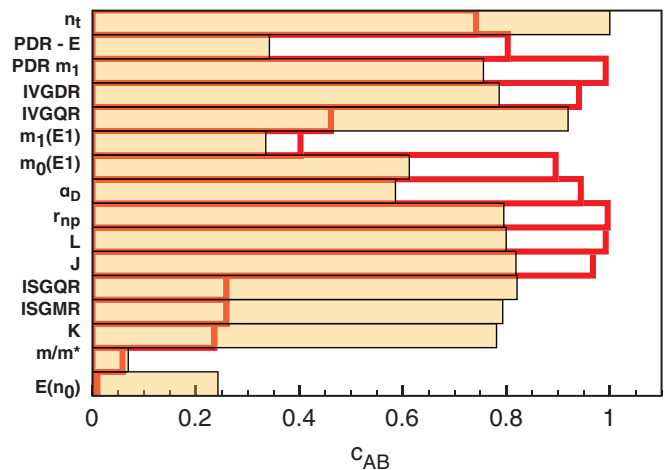


FIG. 1. (Color online) Pearson product-moment correlation coefficients between the neutron star crust liquid-to-solid transition density  $n_t$  (shaded bars - thin lines), and various observables of collective excitations for  $^{208}\text{Pb}$  and nuclear matter properties. The corresponding correlation coefficients for the pressure  $P_t$  are displayed by thick (red) bars.

approach that can be used to identify correlations between physical observables [11,24]. For the purpose of a covariance analysis the DDME-min1 parametrization of the RNEDF has been developed by fitting to ground-state data, that is, binding energies, charge radii, diffraction radii, and surface thickness of 17 spherical nuclei, from  $^{16}\text{O}$  to  $^{214}\text{Pb}$  [25]. Figure 1 shows the corresponding Pearson product-moment correlation coefficients [24] between the neutron star transition density  $n_t$  (and pressure  $P_t$ ) and various quantities that characterize nuclear matter and finite nuclei. The following equilibrium nuclear matter properties are included: the binding energy at saturation density  $E(n_0)$ , the effective mass  $m/m^*$ , the incompressibility  $K$ , the symmetry energy  $J$ , and the slope of the symmetry energy at saturation  $L$  [Eq. (2)]. Characteristic quantities of various modes of excitation of  $^{208}\text{Pb}$  are also taken into consideration: the excitation energies of the isoscalar giant monopole resonance (ISGMR) and isoscalar giant quadrupole resonance (ISGQR), the dipole polarizability ( $\alpha_D$ ), the overall isovector dipole transition strength ( $m_0$ ), and the respective energy-weighted dipole transition strength ( $m_1$ ), the excitation energies of the isovector giant quadrupole resonance (IVGQR) and isovector giant dipole resonance (IVGDR), the  $m_1$  moment (PDR  $m_1$ ), and the excitation energy (PDR - E) of the pygmy dipole strength function. In addition, the neutron-skin thickness ( $r_{np}$ ) in  $^{208}\text{Pb}$  is also included. The present covariance analysis confirms the strong linear correlation between  $n_t$  and the neutron-skin thickness of  $^{208}\text{Pb}$ , as already shown in Ref. [3], and also displays a similar correlation between  $P_t$  and  $r_{np}$ . The results shown in Fig. 1 also indicate that collective excitations in finite nuclei are strongly correlated to the neutron star properties  $n_t$  and  $P_t$ . To constrain possible values of  $(n_t, P_t)$ , of particular interest are observables that simultaneously correlate with both quantities. These include the overall isovector dipole transition strength  $m_0$ , the IVGDR

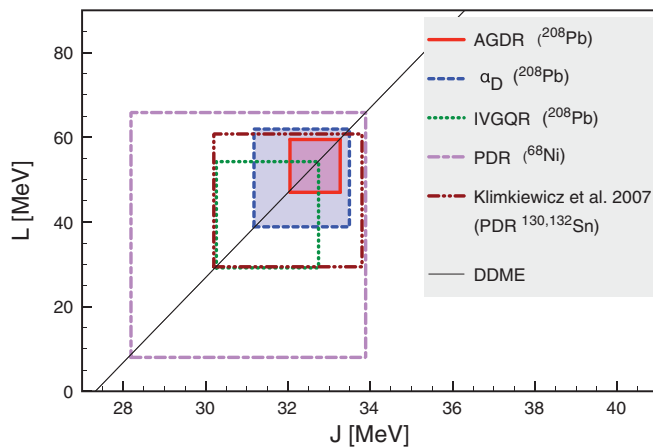


FIG. 2. (Color online) Constraints of the symmetry energy at saturation  $J$  and the slope parameter  $L$ , obtained from a comparison of RNEDF results and data on AGDR [35] and IVGQR [32] excitation energies ( $^{208}\text{Pb}$ ), the dipole polarizability  $\alpha_D$  of  $^{208}\text{Pb}$  [33], and the PDR energy-weighted strength ( $^{68}\text{Ni}$  [34],  $^{130,132}\text{Sn}$  [30]).

and IVGQR excitation energies, the PDR energy-weighted transition strength, and the dipole polarizability.

Figure 1 shows that the liquid-to-solid transition density and pressure are also correlated with the symmetry energy coefficients  $J$  and  $L$ . It is, therefore, interesting to analyze how various excitation modes in nuclei, which limit possible values of  $r_{np}$ , provide constraints on the density dependence of the symmetry energy. Similar studies have recently been performed for different modes of excitation using the framework of energy density functionals (e.g., Refs. [26–28]). In the present analysis a consistent set of RNEDFs that span a range of values  $J = 30\text{--}38$  MeV and  $L = 30\text{--}110.8$  MeV [29] is employed in a calculation of collective excitations. The set of RNEDFs was adjusted to accurately reproduce nuclear matter properties, binding energies, and charge radii of a standard set of spherical nuclei, but with constrained values for the symmetry energy  $J$  and slope parameter  $L$  [29]. These functionals were recently used to constrain the density dependence of the nuclear symmetry energy and the neutron-skin thickness from the observed pygmy dipole strength ( $^{130,132}\text{Sn}$ ) [30], and the anti-analog giant dipole resonance (AGDR) ( $^{208}\text{Pb}$ ) [31]. By performing self-consistent relativistic mean-field calculations for nuclear ground states, and the corresponding RQRPA for collective excitations, we have computed the AGDR and IVGQR excitation energies in  $^{208}\text{Pb}$ , the dipole polarizability  $\alpha_D$  of  $^{208}\text{Pb}$ , and the PDR transition strength in  $^{68}\text{Ni}$ . For the set of RNEDFs, linear correlations are established between the calculated characteristics of collective excitations and the symmetry energy  $J$  and slope parameter  $L$ , in agreement with the results of the covariance analysis shown in Fig. 1. These correlations, together with the corresponding experimental results on the excitation strengths and energies [31–34], provide independent constraints on  $J$  and  $L$ , shown in Fig. 2. For comparison we also include the results of a previous study that was based on the same set of RNEDFs, but used data on the PDR in  $^{130,132}\text{Sn}$  [30]. Figure 2 shows that all calculated excitation

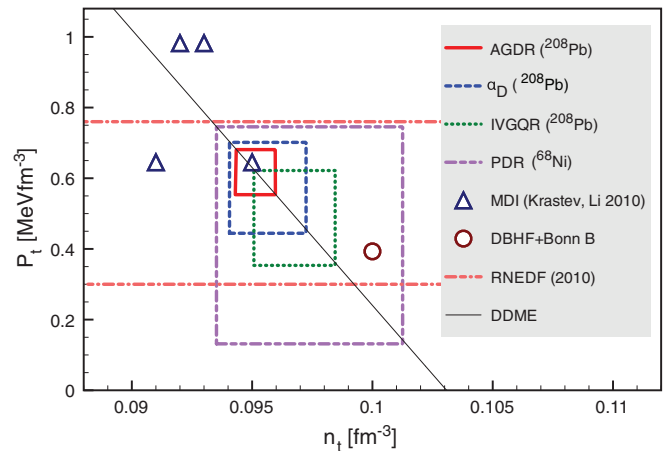


FIG. 3. (Color online) The liquid-to-solid transition pressure  $P_t$  for neutron-rich matter as a function of the transition density  $n_t$ , calculated using the RNEDF and experimental data for AGDR [31] and IVGQR [32] excitation energies ( $^{208}\text{Pb}$ ), the dipole polarizability  $\alpha_D$  ( $^{208}\text{Pb}$ ) [33], and the PDR energy-weighted strength ( $^{68}\text{Ni}$ ) [34]. Previous results shown for comparison include MDI [5,35] and DBHF + Bonn B interactions [36], and the RNEDF calculation [4].

properties consistently constrain possible values of  $J$  and  $L$ , with differences attributed to variations of the experimental uncertainties. It is interesting to note that all results overlap in a narrow region of the  $(J, L)$  plane. The weighted average yields  $J = 32.5 \pm 0.5$  MeV and  $L = 49.9 \pm 4.7$  MeV. More accurate experimental results would, of course, further reduce the uncertainties shown in Fig. 2.

In the next step we have used the same set of RNEDFs to compute the liquid-to-solid transition density and pressure in the thermodynamic approach of Eq. (1). In Fig. 3 the transition pressure  $P_t$  is plotted as a function of the transition density  $n_t$ , and we notice the particular linear dependence predicted by the DDME set of relativistic functionals. The rectangles denote the values of  $P_t$  and  $n_t$ , that is, the corresponding energy density functionals that in a consistent RQRPA calculation reproduce data on collective excitations within experimental uncertainties: the AGDR [31] and IVGQR [32] excitation energies ( $^{208}\text{Pb}$ ), the dipole polarizability  $\alpha_D$  ( $^{208}\text{Pb}$ ) [33], and the PDR energy-weighted strength ( $^{68}\text{Ni}$ ) [34]. One notices that collective excitations provide rather stringent constraints on the possible values of  $P_t$  and  $n_t$ , and there is even a small region in the  $(P_t, n_t)$  plane in which all constraints overlap. Obviously, more accurate measurements of charge-exchange modes and pygmy dipole strength would further reduce the current uncertainties but, nevertheless, the weighted average from the present analysis yields  $n_t = 0.0955 \pm 0.0007$  fm $^{-3}$  and  $P_t = 0.59 \pm 0.05$  MeV fm $^{-3}$ .

For comparison, Fig. 3 also includes constraints on  $(P_t, n_t)$  obtained by other methods, based on modified Gogny (MDI) interactions [5,35], Dirac-Brueckner-Hartree-Fock (DBHF) calculations [36], and RNEDF calculations with constraints from the empirical range for the slope parameter  $L$  and neutron-skin thickness in Sn isotopes and  $^{208}\text{Pb}$  [4]. We note that the RNEDFs used in Ref. [4] differ from the ones employed in the present study. The analysis of Ref. [4] was

based on effective Lagrangians with point-coupling interaction terms rather than the meson-exchange interactions used in this study, and strength and density dependence of the interaction terms were adjusted in a different way. The resulting range  $0.086 \leq n_t < 0.090 \text{ fm}^{-3}$  [4] was slightly below the values deduced in the present work. A previous study based on the  $A18 + \delta v + U1X^*$  interaction predicted a somewhat lower value for the transition density:  $n_t = 0.087 \text{ fm}^{-3}$  [37]; whereas the constraints obtained in the present analysis are consistent with the result based on the nonrelativistic microscopic equation of state of Friedman and Pandharipande [38]:  $n_t = 0.096 \text{ fm}^{-3}$  [39].

In conclusion, we have introduced a method to determine properties of a neutron star crust from a set of observables on collective excitations of finite nuclei. Using covariance analysis based on the RNEDF, it is shown that the neutron star liquid-to-solid phase transition density and pressure are correlated with properties of collective excitations in finite nuclei. A set of RNEDFs characterized by systematic variation of the density dependence of the symmetry energy is used in a self-consistent RPA calculation of the AGDR and

IVGQR excitation energies ( $^{208}\text{Pb}$ ), the dipole polarizability  $\alpha_D$  ( $^{208}\text{Pb}$ ), and the PDR energy-weighted strength ( $^{68}\text{Ni}$ ). Using the thermodynamic method, the same set of RNEDFs predicts a particular linear dependence of the phase transition density  $n_t$  and pressure  $P_t$  at the inner edge between the liquid core and the solid crust of a neutron star. By comparing the corresponding RPA theoretical values on collective excitations in nuclei with experimental data, rather stringent constraints on the possible values are obtained:  $n_t = 0.0955 \pm 0.0007 \text{ fm}^{-3}$  and  $P_t = 0.59 \pm 0.05 \text{ MeV fm}^{-3}$ . Although the present analysis is based on a single family of RNEDFs, it introduces a novel method and demonstrates the feasibility of the proposed approach. Further extensive studies using a larger set of nonrelativistic and relativistic functionals, including also other modes of excitation, will provide more robust quantitative estimates of the liquid-to-solid transition density and pressure. This method crucially depends on experimental uncertainties of observables that characterize collective modes of excitation and, therefore, accurate measurements are necessary to further constrain the structure of the neutron star crust.

- 
- [1] P. Haensel, A. Y. Potekhin, and D. G. Yakovlev, *Neutron Stars I: Equation of State and Structure* (Springer-Verlag, New York, 2007).
- [2] J. M. Lattimer and M. Prakash, *Phys. Rep.* **333-334**, 121 (2000).
- [3] C. J. Horowitz and J. Piekarewicz, *Phys. Rev. Lett.* **86**, 5647 (2001).
- [4] Ch. C. Moustakidis, T. Nikšić, G. A. Lalazissis, D. Vretenar, and P. Ring, *Phys. Rev. C* **81**, 065803 (2010).
- [5] J. Xu, L. W. Chen, B. A. Li, and H. R. Ma, *Astrophys. J.* **697**, 1549 (2009).
- [6] C. Ducoin, J. Margueron, C. Providencia, and I. Vidana, *Phys. Rev. C* **83**, 045810 (2011).
- [7] A. W. Steiner, M. Prakash, J. M. Lattimer, and P. J. Ellis, *Phys. Rep.* **411**, 325 (2005).
- [8] J. Carriere, C. J. Horowitz, and J. Piekarewicz, *Astrophys. J.* **593**, 463 (2003).
- [9] C. J. Horowitz and J. Piekarewicz, *Phys. Rev. C* **66**, 055803 (2002).
- [10] F. J. Fattoyev and J. Piekarewicz, *Phys. Rev. C* **82**, 025810 (2010).
- [11] F. J. Fattoyev and J. Piekarewicz, *Phys. Rev. C* **86**, 015802 (2012).
- [12] S. Abrahamyan *et al.*, *Phys. Rev. Lett.* **108**, 112502 (2012).
- [13] D. Savran, T. Aumann, and A. Zilges, *Prog. Part. Nucl. Phys.* **70**, 210 (2013).
- [14] C. J. Pethick, D. G. Ravenhall, and C. P. Lorenz, *Nucl. Phys. A* **584**, 675 (1995); F. Douchin and P. Haensel, *Phys. Lett. B* **485**, 107 (2000).
- [15] C. Ducoin, Ph. Chomaz, and F. Gulminelli, *Nucl. Phys. A* **789**, 403 (2007).
- [16] J. M. Lattimer and M. Prakash, *Phys. Rep.* **442**, 109 (2007).
- [17] S. Kubis, *Phys. Rev. C* **76**, 025801 (2007).
- [18] A. Worley, P. G. Krastev, and B. A. Li, *Astrophys. J.* **685**, 390 (2008).
- [19] T. Nikšić, D. Vretenar, P. Finelli, and P. Ring, *Phys. Rev. C* **66**, 024306 (2002).
- [20] N. Paar *et al.*, *Rep. Prog. Phys.* **70**, 691 (2007).
- [21] R. J. Furnstahl, *Nucl. Phys. A* **706**, 85 (2002).
- [22] M. Centelles, X. Roca-Maza, X. Vinas, and M. Warda, *Phys. Rev. Lett.* **102**, 122502 (2009).
- [23] F. J. Fattoyev and J. Piekarewicz, *Phys. Rev. C* **84**, 064302 (2011).
- [24] P.-G. Reinhard and W. Nazarewicz, *Phys. Rev. C* **81**, 051303(R) (2010).
- [25] X. Roca-Maza, N. Paar, and G. Coló, [arXiv:1406.1885](https://arxiv.org/abs/1406.1885) [J. Phys. G (2014) (to be published)].
- [26] A. Carbone, G. Colò, A. Bracco, L. G. Cao, P. F. Bortignon, F. Camera, and O. Wieland, *Phys. Rev. C* **81**, 041301(R) (2010).
- [27] M. B. Tsang *et al.*, *Phys. Rev. C* **86**, 015803 (2012).
- [28] X. Roca-Maza *et al.*, *Phys. Rev. C* **87**, 034301 (2013).
- [29] D. Vretenar, T. Nikšić, and P. Ring, *Phys. Rev. C* **68**, 024310 (2003).
- [30] A. Klimkiewicz *et al.*, *Phys. Rev. C* **76**, 051603(R) (2007).
- [31] A. Krasznahorkay *et al.*, [arXiv:1311.1456v2](https://arxiv.org/abs/1311.1456v2).
- [32] S. S. Henshaw, M. W. Ahmed, G. Feldman, A. M. Nathan, and H. R. Weller, *Phys. Rev. Lett.* **107**, 222501 (2011).
- [33] A. Tamii *et al.*, *Phys. Rev. Lett.* **107**, 062502 (2011).
- [34] O. Wieland, A. Bracco, F. Camera *et al.*, *Phys. Rev. Lett.* **102**, 092502 (2009).
- [35] P. G. Krastev and B. A. Li, [arXiv:1001.0353](https://arxiv.org/abs/1001.0353).
- [36] F. Sammarruca and P. Liu, *Phys. Rev. C* **79**, 057301 (2009); F. Sammarruca, [arXiv:1002.0146](https://arxiv.org/abs/1002.0146).
- [37] A. Akmal, V. R. Pandharipande, and D. G. Ravenhall, *Phys. Rev. C* **58**, 1804 (1998).
- [38] B. Friedman and V. R. Pandharipande, *Nucl. Phys. A* **361**, 502 (1981).
- [39] C. P. Lorenz, D. G. Ravenhall, and C. J. Pethick, *Phys. Rev. Lett.* **70**, 379 (1993).